

Original Article

DOI 10.1007/s12206-020-0605-6

Keywords:

- Transfer matrix method
- Rotating tapered beam
- Euler-Bernoulli beam
- Centrifugal force
- Contribution rate

Correspondence to:

Jung Youn Lee
jylee@kgu.ac.kr

Citation:

Lee, J. W., Lee, J. Y. (2020). Free vibration analysis of a rotating double-tapered beam using the transfer matrix method. Journal of Mechanical Science and Technology 34 (7) (2020) 2731–2744.
<http://doi.org/10.1007/s12206-020-0605-6>

Received February 19th, 2020

Revised April 9th, 2020

Accepted April 16th, 2020

† Recommended by Editor
No-cheol Park

Free vibration analysis of a rotating double-tapered beam using the transfer matrix method

Jung Woo Lee and Jung Youn Lee

Department of Mechanical System Engineering, Kyonggi University, 154-42, Gwanggyosan-ro, Yeongtong-gu, Suwon-si, Gyeonggi-do 16227, Korea

Abstract In this study, a transfer matrix method is developed to analyze the effect of the centrifugal force on the natural frequencies of a rotating double-tapered beam, whose cross-sections have linearly reduced height and width. The root of the differential equation is determined based on the Bernoulli-Euler theory and the effects of the hub radius, taper ratio, and rotation speed, by applying the Frobenius method. In particular, the effect of the centrifugal forces is analyzed based on the relationship between the bending and additional strain energies generated by centrifugal stiffening. The shape function of the displacements depends on the variations in the taper ratio and rotation speed. In addition, the strain energies are varied. Various examples are presented to demonstrate the influences of the strain energies. Furthermore, the effects of the centrifugal force on the natural frequencies of the rotating double-tapered beam are investigated by analyzing the variation in the predicted strain energy.

1. Introduction

Many researchers have investigated rotating and non-uniform beams [1-6] to obtain more accurate results for practical engineering designs. In addition, they have studied various problems such as buckling [7, 8] and Coriolis effects [9] and the effects of the centrifugal force [10-13], gravity [14], rotary inertia, and shear deformations [15-22]. The assumption of shape functions for similar problems enhance the result accuracy and simplify the computation processes [23-28]. The truncated polynomial series and Bessel functions are typical examples used to compute the roots of differential equations to determine natural frequencies more accurately. However, the Bessel functions cannot be used for all problems [29]. Truncated polynomial series such as the Frobenius and Tayler methods can yield exact solutions when the number of terms of the power series that are displayed is infinity. Nevertheless, their application in practical calculations is infeasible [30, 31]. Thus, the accuracy of results computed with the Frobenius method depends on the number of terms used in the truncated polynomial series [32, 33].

The Frobenius method has been studied in conjunction with various other methods such as transfer matrices [34], dynamic stiffness matrices [35], and linearization approaches [36]. It has been widely applied to solve the dynamic characteristics of beams experiencing centrifugal force and with uniform tapers. Studies on the effect of the centrifugal force have focused on obtaining more accurate results. Moreover, the effect of the centrifugal force on the natural frequencies has been generally investigated based on the frequency ratio [37-42].

A new analytical method for identifying these effects based on the influence of the strain energies was proposed by Lee and Lee [41]. They analyzed the influence of the centrifugal force on the natural frequencies of a rotating single-tapered beam. The classification of the influences of the strain energies enables a more accurate analysis of the centrifugal force's effect than the use of the frequency ratio does. The authors briefly mentioned the influence of the strain energies on the centrifugal force. The influence of the strain energies on the natural frequencies of a rotating double-tapered beam cannot be analyzed with their method. Therefore,

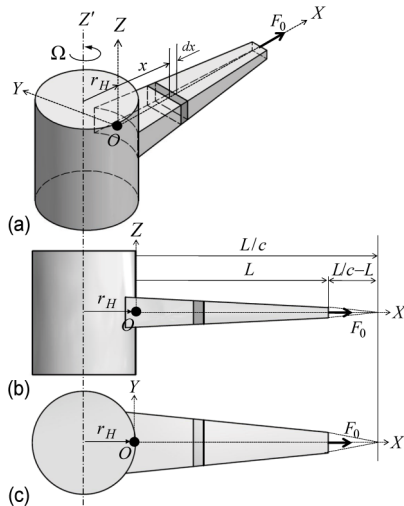


Fig. 1. Notation and coordinate system used for rotating double-tapered Bernoulli-Euler beam: (a) Geometry of tapered beam; (b) side view; (c) top view.

an analytical method capable of classifying the effect of strain energies on the natural frequencies of a rotating double-tapered beam is proposed in this paper.

The main objective of this research study is to develop a transfer matrix method (TMM) to analyze the dynamics characteristics of a rotating double-tapered beam. The Frobenius method is used to determine the roots of the differential equation. Furthermore, the effect of centrifugal stiffening on the natural frequencies of the beam is investigated as a contribution rate of the strain energy. The contribution rate is predicted by equating the maximal strain and kinetic energies. The maximal kinetic energies are normalized to analyze the contribution rate of the strain energies. The TMM developed can be used to compute the eigenpairs of a rotating double-tapered beam. In addition, it is employed to determine the shape function of the displacements required for computing the contribution rate. The effects of the taper ratio, hub radius, and rotation speed with regard to centrifugal stiffening are examined through various examples. They are analyzed as the rates of the strain energy contributed to the natural frequency under each condition.

2. Theory

The beam examined in this study is assumed to have a sufficient length with regard to the cross-sectional dimensions. In addition, the rotary inertia and shear deformations are omitted. The notation and coordinate systems in Fig. 1 are used to solve for the bending vibration of the rotating double-tapered Bernoulli-Euler beam: XYZ is the global coordinate system, L is the total length of the beam element, and c is the taper ratio; Z' is the central axis of rotation, Ω is the rotation speed, r_H is the hub radius, dx is the length of the infinitesimal element, x is the distance from point 0 to the infinitesimal component, and F_0 is the axial force.

The differential equation, bending moment, and shear force for the bending vibration of a rotating double-tapered beam can be determined by different variational principles. The strain (U) and kinetic (T) energies are expressed as follows [35, 41]:

$$U = U_B + U_F \\ = \frac{1}{2} \int_0^L EI(x)(w'')^2 dx + \frac{1}{2} \int_0^L F(x)(w')^2 dx \quad (1)$$

and

$$T = \frac{1}{2} \int_0^L m(x)(\dot{w})^2 dx \quad (2)$$

where $EI(x)$ and $m(x)$ are the variations in the bending stiffness and mass per unit length, respectively, owing to the taper ratio. $I(x)$ is the variation in the geometric moments of inertia of the beam cross-section with respect to the taper ratio, E the elastic modulus of the beam element, and $w(w(x,t))$ the in-plane bending displacement. The prime and dot denote differentiation with respect to the distance x and time t , respectively. The variations in the bending stiffness and mass of a double-tapered beam can be expressed as follows:

$$EI(x) = EI_0 \left(1 - c \frac{x}{L}\right)^4 = EI_0 (1 - \zeta)^4 \quad (3)$$

and

$$m(x) = m_0 \left(1 - c \frac{x}{L}\right)^2 = m_0 (1 - \zeta)^2 \quad (4)$$

where $\zeta = c\bar{x}$, and $\bar{x}(=x/L)$ is non-dimensional coordinate. EI_0 and m_0 are the bending stiffness and mass per unit length, respectively, of a uniform beam ($c = 0$).

As shown in Fig. 1, $F(x)$ is the centrifugal force at a distance x including the axial force acting at the end of the beam:

$$F(x) = \int_x^L m(x)\Omega^2(x + r_H)dx + F_0 \quad (5)$$

where the axial force F_0 can be considered zero.

By substituting Eqs. (3) and (4) into Eq. (5) (by integrating this equation), the centrifugal force $F(\zeta)$ can be expressed as follows:

$$F(\zeta) = m_0 \Omega^2 \left\{ \frac{L^2}{c^2} \left(\frac{1}{4} c^4 - \frac{2}{3} c^3 + \frac{1}{2} c^2 \right) \right. \\ \left. + r_H \frac{L}{c} \left(\frac{1}{3} c^3 - c^2 + c \right) - \frac{L^2}{c^2} \left(\frac{\zeta^4}{4} - \frac{2\zeta^3}{3} + \frac{\zeta^2}{2} \right) \right. \\ \left. - r_H \frac{L}{c} \left(\frac{1}{3} \zeta^3 - \zeta^2 + \zeta \right) + F_0 \right\} \quad (6)$$

Differentiating Eq. (6) with respect to ζ results in the following expression:

$$F'(\zeta) = -m_0\Omega^2 \left(\frac{L}{c} (\zeta^3 - 2\zeta^2 + \zeta) + r_H (\zeta^2 - 2\zeta + 1) \right). \quad (7)$$

Furthermore, harmonic vibrations with angular frequencies (ω) are considered:

$$w(x,t) = W(x) \cos \omega t \quad (8)$$

where $W(x)$ represents the amplitudes of $w(x,t)$.

With the aid of Eqs. (1), (2) and (8), the maximal strain and kinetic energies can be expressed as follows:

$$\begin{aligned} U_{\max} \\ = \frac{1}{2} \int_0^L EI(x)(W''(x))^2 dx + \frac{1}{2} \int_0^L F(x)(W'(x))^2 dx \end{aligned} \quad (9)$$

and

$$T_{\max} = \frac{1}{2} \int_0^L m(x)\omega^2(W(x))^2 dx. \quad (10)$$

By equating Eqs. (9) and (10), the relationship between the two energies can be defined as follows [41]:

$$\begin{aligned} \omega^2 &= S_B + S_F \\ &= \sum_{i=0}^n \frac{EI(x_i)(W''(x_i))^2}{m(x_i)(W(x_i))^2} + \sum_{i=0}^n \frac{F(x_i)(W'(x_i))^2}{m(x_i)(W(x_i))^2} \end{aligned} \quad (11)$$

where S_B is the bending strain energy at the normalized maximal kinetic energy, and S_F is the additional strain energy caused by centrifugal stiffening.

From Eq. (11), the contribution rate of the strain energies on the eigenfrequencies of a rotating double-tapered beam can be computed as follows:

$$C_B + C_F = 1 \quad (12)$$

where $C_B (= S_B / \omega^2)$ is the contribution rate of the bending strain energy to the natural frequencies. $C_F (= S_F / \omega^2)$ is the contribution rate of the strain energy generated by the centrifugal force. The unknown parameters are the shape functions of the displacements (i.e., W , W' and W'').

The contribution rate of the strain energies can be obtained if the bending displacement W is known. W can be deduced from the differential equation as described below.

The differential equation of the variational principle can be expressed as follows [35, 41]:

$$(EI(x)w'')'' - (F(x)w')' + m(x)\ddot{w} = 0. \quad (13)$$

Moreover, the shear force and bending moment can be defined as follows [35, 41]:

$$V(x,t) = (EI(x)w'')' - F(x)w' \quad (14)$$

and

$$M(x,t) = -EI(x)w'' \quad (15)$$

where $V(x,t)$ is the shear force and $M(x,t)$ is the bending moment.

By substituting Eq. (8) into Eq. (13), the equation can be re-expressed as follows:

$$\begin{aligned} EI(x)W''' + 2EI'(x)W'' + (EI''(x) - F(x))W'' \\ - F'(x)W' - \omega^2 m(x)W = 0 \end{aligned} \quad (16)$$

where $W = W(x)$.

By substituting Eqs. (3), (4), (6) and (7) into Eq. (16), the differential equation can be re-expressed in a nondimensional form:

$$\begin{aligned} (1-\zeta)^4 W''' - 8(1-\zeta)^3 W''' \\ + \left\{ 12(1-\zeta)^2 + D_1 \left(\frac{\zeta^4}{4} - \frac{2\zeta^3}{3} + \frac{\zeta^2}{2} \right) \right. \\ \left. + D_2 \left(\frac{1}{3}\zeta^3 - \zeta^2 + \zeta \right) + D_3 \right\} W'' \\ + \left\{ D_1(\zeta^3 - 2\zeta^2 + \zeta) + D_2(\zeta^2 - 2\zeta + 1) \right\} W' \\ + D_4(1-\zeta)^2 W = 0 \end{aligned} \quad (17)$$

where

$$\begin{aligned} D_1 &= \frac{m_0\Omega^2 L^4}{EI_0 c^4}, \quad D_2 = r_H \frac{m_0\Omega^2 L^3}{EI_0 c^3} \\ D_3 &= -D_1 \left(\frac{c^4}{4} - \frac{2c^3}{3} + \frac{c^2}{2} \right) - D_2 \left(\frac{c^3}{3} - c^2 + c \right) \\ &- \frac{F_0 L^2}{EI_0 c^2}, \quad D_4 = -\frac{m_0 \omega^2 L^4}{EI_0 c^4}. \end{aligned} \quad (18)$$

Eq. (18) can be expressed as follows:

$$\begin{aligned} (\zeta^4 - 4\zeta^3 + 6\zeta^2 - 4\zeta + 1)W''' \\ + (8\zeta^3 - 24\zeta^2 + 24\zeta - 8)W'' \\ + \left\{ \bar{D}_1\zeta^4 + \bar{D}_2\zeta^3 + \bar{D}_3\zeta^2 + \bar{D}_4\zeta + \bar{D}_5 \right\} W'' \\ + \left\{ \bar{D}_6\zeta^3 + \bar{D}_7\zeta^2 + \bar{D}_8\zeta + \bar{D}_9 \right\} W' + \bar{D}_{10}(1-\zeta)^2 W \\ = 0 \end{aligned} \quad (19)$$

where

$$\begin{aligned}\bar{D}_1 &= \frac{D_1}{4}, \quad \bar{D}_2 = \left(\frac{D_2}{3} - \frac{2D_1}{3} \right), \quad \bar{D}_3 = \left(\frac{D_1}{2} - D_2 + 12 \right), \\ \bar{D}_4 &= (D_2 - 24), \quad \bar{D}_5 = (D_3 + 12), \\ \bar{D}_6 &= D_1, \quad \bar{D}_7 = (D_2 - 2D_1), \quad \bar{D}_8 = (D_1 - 2D_2), \\ \bar{D}_9 &= D_2, \quad \bar{D}_{10} = D_4\end{aligned}\quad (20)$$

The roots of Eq. (19) can be computed using the Frobenius method. The following expression can be considered the general solution of Eq. (19):

$$W(\zeta, k) = \sum_{i=0}^{\infty} a_{i+1}(k) \zeta^{k+i}. \quad (21)$$

When Eq. (21) is substituted into Eq. (19), the indicial equation and recurrence relationship of the Frobenius coefficients can be determined as follows:

$$k(k-1)(k-2)(k-3) = 0 \quad (22)$$

and

$$\begin{aligned}a_{i+6}(k) &= \frac{4(k+i+3)}{(k+i+5)} a_{i+5}(k) \\ &\quad - \frac{6(k+i+4)(k+i+1)+\bar{D}_5}{(k+i+4)(k+i+5)} a_{i+4}(k) \\ &\quad - \frac{\{\bar{D}_4-4(k+i+5)\}(k+i)}{(k+i+3)(k+i+4)(k+i+5)} a_{i+3}(k) \\ &\quad - \left[\frac{\{(k+i+6)(k+i-1)+\bar{D}_3\}(k+i+1)(k+i)}{(k+i+2)(k+i+3)(k+i+4)(k+i+5)} \right. \\ &\quad \left. + \frac{\bar{D}_8(k+i+1)+\bar{D}_{10}}{(k+i+2)(k+i+3)(k+i+4)(k+i+5)} \right] a_{i+2}(k) \\ &\quad - \frac{\{\bar{D}_2(k+i-1)+\bar{D}_7\}(k+i)-2\bar{D}_{10}}{(k+i+2)(k+i+3)(k+i+4)(k+i+5)} a_{i+1}(k) \\ &\quad - \frac{\{\bar{D}_1(k+i-2)+\bar{D}_6\}(k+i-1)+\bar{D}_{10}}{(k+i+2)(k+i+3)(k+i+4)(k+i+5)} a_i(k)\end{aligned}\quad (23)$$

where

$$\begin{aligned}a_1 &= 1, \quad a_2 = \frac{4(k-1)}{(k+1)} a_1, \quad a_3 = \frac{4k}{(k+2)} a_2 \\ &\quad - \frac{6(k-2)(k+1)+\bar{D}_5}{(k+1)(k+2)} a_1, \\ a_4 &= \frac{4(k+1)}{(k+3)} a_3 - \frac{6(k+2)(k-1)+\bar{D}_5}{(k+2)(k+3)} a_2 \\ &\quad - \frac{\{\bar{D}_4-4(k+3)(k-2)\}(k-1)+\bar{D}_9}{(k+1)(k+2)(k+3)} a_1,\end{aligned}\quad (24)$$

$$\begin{aligned}a_5 &= \frac{4(k+2)}{(k+4)} a_4 - \frac{6(k+3)k+\bar{D}_5}{(k+3)(k+4)} a_3 \\ &\quad - \frac{\{\bar{D}_4-4(k+4)(k-1)\}k+\bar{D}_9}{(k+2)(k+3)(k+4)} a_2 \\ &\quad - \frac{\{(k+5)(k-2)+\bar{D}_3\}k(k-1)+\bar{D}_8k+\bar{D}_{10}}{(k+1)(k+2)(k+3)(k+4)} a_1, \\ a_6 &= \frac{4(k+3)}{(k+4)} a_5 - \frac{6(k+4)(k+1)+\bar{D}_5}{(k+4)(k+5)} a_4 \\ &\quad - \frac{\{\bar{D}_4-4(k+5)k\}(k+1)+\bar{D}_9}{(k+3)(k+4)(k+5)} a_3 \\ &\quad - \frac{\{(k+6)(k-1)+\bar{D}_3\}(k+1)k+\bar{D}_8(k+1)+\bar{D}_{10}}{(k+2)(k+3)(k+4)(k+5)} a_2 \\ &\quad - \frac{\{\bar{D}_2(k-1)+\bar{D}_7\}k-2\bar{D}_{10}}{(k+2)(k+3)(k+4)(k+5)} a_1.\end{aligned}$$

In addition, the four roots of the indicial equation in Eq. (22) are $k = 0, 1, 2$, and 3 . The solution of the differential equation multiplied by four arbitrary constants for the four k values can be expressed as follows:

$$W(\zeta) = A_1 f(\zeta, 0) + A_2 f(\zeta, 1) + A_3 f(\zeta, 2) + A_4 f(\zeta, 3) \quad (25)$$

where A_1, A_2, A_3 , and A_4 are constants. $f(\zeta, k)$ can be expressed as follows:

$$f(\zeta, k) = \sum_{i=0}^{\infty} a_{i+1}(k) \zeta^{k+i}. \quad (26)$$

The slope of the deformation curve (Φ) is obtained as follows by differentiating Eq. (25):

$$\begin{aligned}\Phi &= \frac{c}{L} \frac{dW(\zeta)}{d\zeta} \\ &= \frac{c}{L} \{A_1 f'(\zeta, 0) + A_2 f'(\zeta, 1) + A_3 f'(\zeta, 2) + A_4 f'(\zeta, 3)\}.\end{aligned}\quad (27)$$

The bending moment and shear force can be obtained as follows by substituting Eq. (8) and appropriate differentiations of Eq. (25), into Eqs. (14) and (15):

$$M = N_1 (1-\zeta)^4 \frac{d^2 W(\zeta)}{d\zeta^2} \quad (28)$$

and

$$\begin{aligned}V &= N_2 \left\{ (1-\zeta)^4 \frac{d^3 W(\zeta)}{d\zeta^3} - 4(1-\zeta)^3 \frac{d^2 W(\zeta)}{d\zeta^2} \right. \\ &\quad \left. + (\bar{D}_1 \zeta^4 + \bar{D}_2 \zeta^3 + \bar{D}_{11} \zeta^2 + \bar{D}_{12} \zeta + \bar{D}_{13}) \frac{dW(\zeta)}{d\zeta} \right\}\end{aligned}\quad (29)$$

Table 1. Comparison of the results for the first three non-dimensional natural frequencies when $c = 0.5$ and $\bar{r}_H = 0$.

Ω	N_{ps}	Non-dimensional natural frequency					
		$\bar{\omega}_1$		$\bar{\omega}_2$		$\bar{\omega}_3$	
		Present	Banerjee [35]	Present	Banerjee [35]	Present	Banerjee [35]
0	90	4.62515	4.62515	19.5476	19.5476	48.5789	48.5789
5	90	7.29014	7.29014	22.6360	22.6360	51.6918	51.6918
10	100	11.9415	11.9415	30.0299	30.0299	60.0399	60.0399

where

$$\begin{aligned} N_1 &= -\frac{EI_0 c^2}{L^2}, \quad N_2 = \frac{EI_0 c^3}{L^3}, \\ \bar{D}_{11} &= (\bar{D}_3 - 12), \quad \bar{D}_{12} = (\bar{D}_4 + 24), \quad \bar{D}_{13} = (\bar{D}_5 - 12). \end{aligned} \quad (30)$$

The displacements and forces are now known. However, the constants $A_1 - A_4$ in Eq. (25) are unknown. The TMM is employed to determine these constants based on the boundary conditions. The transfer matrix for the dynamic behavior analysis of a rotating double-tapered beam can be derived as described below.

The nondimensional distance \bar{x} of the beam elements at the ends of the tapered beam are $\bar{x} = 0$ and $\bar{x} = L$. Therefore, when $\bar{x} = 0$ is substituted into Eqs. (25) and (27)-(29), the state vector (Z_0) at $\bar{x} = 0$ is expressed as

$$Z_0 = CA \quad (31)$$

where $Z_0 = [W, \Theta, M, V]^T_{\bar{x}=0}$, and $A = [A_1, A_2, A_3, A_4]^T$. The components of the matrix C are defined as follows:

$$\begin{aligned} C_{1j} &= \sum_{j=1}^4 f(0, j-1), \quad C_{2j} = \frac{c}{L} \sum_{j=1}^4 f'(0, j-1), \\ C_{3j} &= N_1 \sum_{j=1}^4 f''(0, j-1), \\ C_{4j} &= N_2 \left(\sum_{j=1}^4 f'''(0, j-1) - 4 \sum_{j=1}^4 f''(0, j-1) \right. \\ &\quad \left. + \bar{D}_{13} \sum_{j=1}^4 f'(0, j-1) \right). \end{aligned} \quad (32)$$

From Eq. (31), the unknown constants A are expressed as

$$A = C^{-1} Z_0. \quad (33)$$

By substituting $\bar{x} = 1$ into Eqs. (25) and (27)-(29), the state vector Z_1 can be expressed as follows:

$$Z_1 = QA \quad (34)$$

where $Z_1 = [W, \Theta, M, V]^T_{\bar{x}=1}$. The components of the matrix Q are obtained by

$$\begin{aligned} Q_{1j} &= \sum_{j=1}^4 f(c, j-1), \quad Q_{2j} = \frac{c}{L} \sum_{j=1}^4 f'(c, j-1), \\ Q_{3j} &= N_1 (1-c)^4 \sum_{j=1}^4 f''(c, j-1), \\ Q_{4j} &= N_2 \left((1-c)^4 \sum_{j=1}^4 f'''(c, j-1) \right. \\ &\quad \left. - 4(1-c)^3 \sum_{j=1}^4 f''(c, j-1) \right. \\ &\quad \left. + (\bar{D}_1 c^4 + \bar{D}_2 c^3 + \bar{D}_1 c^2 + \bar{D}_{12} c + \bar{D}_{13}) \sum_{j=1}^4 f'(c, j-1) \right). \end{aligned} \quad (35)$$

Based on Eqs. (33) and (34), the state vectors Z_0 and Z_1 exhibit the following relationship:

$$Z_1 = TZ_0 \quad (36)$$

where $T = QC^{-1}$ is a transfer matrix.

The constants $A_1 - A_4$ can be computed based on the transfer matrix determined (T). The procedure for obtaining the frequency determinant of 4×4 transfer matrices have been discussed in many studies [27, 34]. Thus, the contribution rate of the strain energies to the natural frequencies of a rotating double-tapered beam can be predicted using Eq. (12).

3. Results and discussion

To demonstrate the accuracy of the proposed TMM, the computed results are compared with the nondimensional natural frequencies reported in Banerjee et al. [35] for rotation speeds of 0, 5, and 10 and a taper ratio of 0.5. The comparison results for the rotating double-tapered beam are listed in Table 1. They agree well. The effect of the centrifugal force on the first three mode shapes of the rotating double-tapered beam in clamped-free (C-F) end condition is illustrated in Fig. 2. N_{ps} is the number of terms used in the power series.

Moreover, the effects of the bending and additional strain energies by centrifugal stiffening, on the nondimensional natural frequencies of rotating uniform beams in C-F end condition are compared with the results discussed in Lee and Lee [41]. The results for the rotation speeds of 0, 5, and 10 are listed in Table 2. The comparison results reveal a high agreement between the present and previous works. NF_1 represents the result calculated using the TMM in Eq. (36) (computed with one element). NF_2 is the predicted result based on Eq. (11).

Table 2. Comparisons of the contribution rate of strain energies on the first four non-dimensional natural frequencies of rotating uniform beams with clamped-free end condition: $\bar{r}_H = 0$, $c = 0$.

Ω	Non-dimensional natural frequency and contribution rate							
	$\bar{\omega}_1$		$\bar{\omega}_2$		$\bar{\omega}_3$		$\bar{\omega}_4$	
	Present	Lee [41]	Present	Lee [41]	Present	Lee [41]	Present	Lee [41]
0	NF_1	3.5175	3.5161	22.0297	22.0338	61.6724	61.6945	120.8475
	C_B	1.0000	1.0000	1.0000	1.0000	1.0000	1.0000	1.0000
	C_F	0.0000	0.0000	0.0000	0.0000	0.0000	0.0000	0.0000
	NF_2	3.5175	3.5161	22.0296	22.0338	61.6720	61.6945	120.8468
	Diff(%)	0.0004	0.0000	0.0005	0.0000	0.0005	0.0005	0.0001
5	NF_1	6.4506	6.4496	25.4407	25.4454	65.1794	65.2024	124.5109
	C_B	0.3165	0.3164	0.7541	0.7541	0.8976	0.8976	0.9433
	C_F	0.6835	0.6836	0.2459	0.2459	0.1024	0.1024	0.0567
	NF_2	6.4246	6.4236	25.3814	25.3862	65.1286	65.1518	124.4644
	Diff(%)	0.4029	0.4030	0.2331	0.2327	0.0780	0.0775	0.0369
10	NF_1	11.2032	11.2024	33.6336	33.6397	74.6214	74.6467	134.8255
	C_B	0.1332	0.1331	0.4389	0.4389	0.6914	0.6914	0.8084
	C_F	0.8668	0.8669	0.5611	0.5611	0.3086	0.3086	0.1916
	NF_2	11.1535	11.1526	33.4468	33.4530	74.4377	74.4632	134.6522
	Diff(%)	0.4442	0.4445	0.5553	0.5551	0.2462	0.2458	0.1285

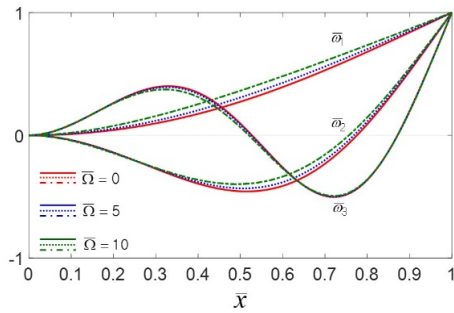


Fig. 2. Effect of centrifugal stiffening on first three mode shapes of rotating double-tapered beam with cantilever end condition.

For example, in Lee and Lee [41], the nondimensional distance $\bar{x}(x/L)$ in the computation of the displacements (W , W' , and W'') using Eq. (11) is divided into 100 equal parts. Diff.(%) is the percentage difference of the results predicted with Eqs. (11) and (36). Further investigations are conducted because the analysis of the influence of the strain energies on the natural frequencies of the rotating double-tapered beam has been successful.

3.1 Effects of centrifugal stiffening

In this subsection, the effects of centrifugal stiffening on the nondimensional natural frequencies of the three beam types (uniform beam, single-tapered beam, and double-tapered beam) are discussed.

The single-tapered beam has a cross-section with a linearly reduced height, and the double-tapered beam has cross-sections with linearly reduced width and height. The contribu-

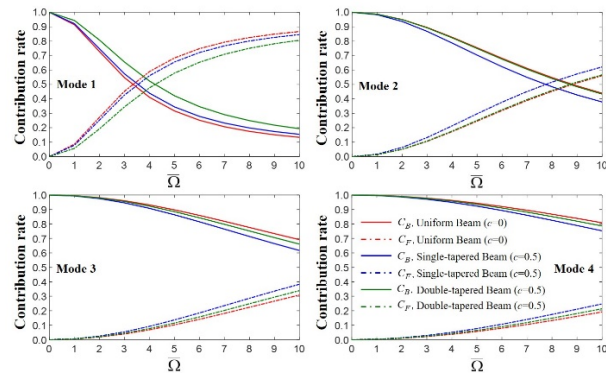


Fig. 3. Variations in contribution rates of strain energies at nondimensional natural frequencies of the three beam types owing to centrifugal stiffening.

tions of the strain energies to the natural frequencies of the rotating single-tapered beam are based on the results in Lee and Lee [41]. The tapered ratio is set to 0.5, and the rotational speeds are increased from 0 to 10 at steps of 1. The results of the rotating uniform and tapered beams are listed in Table 3. Fig. 3 compares the three beam types.

As shown in Fig. 3, the effect of the centrifugal force on the first mode of the rotating uniform beam is strong. Meanwhile, the second, third, and forth modes exhibit the weakest effect of the centrifugal force compared with those of the other beam types.

In addition, the effect of the centrifugal force on the rotating single-tapered beam is larger than those on the other beam types in the second, third, and forth modes.

Identical phenomena are observed with the frequency ratios in Fig. 4. However, the investigation of the effect of the cen-

Table 3. Contribution rates of strain energies at nondimensional natural frequencies of rotating uniform and tapered beams with clamped-free end condition with respect to variations in rotation speed.

$\bar{\Omega}$	Non-dimensional natural frequency and Contribution rate												
	Present								Lee and Lee [41]				
	$c = 0, \bar{r}_H = 0$				$c = 0.5, \bar{r}_H = 0$				$c = 0.5, \bar{r}_H = 0$				
	$\bar{\omega}_1$	$\bar{\omega}_2$	$\bar{\omega}_3$	$\bar{\omega}_4$	$\bar{\omega}_1$	$\bar{\omega}_2$	$\bar{\omega}_3$	$\bar{\omega}_4$	$\bar{\omega}_1$	$\bar{\omega}_2$	$\bar{\omega}_3$	$\bar{\omega}_4$	
0	NF_1	3.5175	22.0297	61.6724	120.8475	4.6252	19.5476	48.5789	91.8128	3.8238	18.3173	47.2648	90.4505
	C_B	1.0000	1.0000	1.0000	1.0000	1.0000	1.0000	1.0000	1.0000	1.0000	1.0000	1.0000	1.0000
	C_F	0.0000	0.0000	0.0000	0.0000	0.0000	0.0000	0.0000	0.0000	0.0000	0.0000	0.0000	0.0000
	NF_2	3.5175	22.0296	61.6720	120.8468	4.6179	19.4924	48.4196	91.4926	3.8155	18.2610	47.1035	90.1271
1	NF_1	3.6831	22.1762	61.8169	120.9964	4.7641	19.6803	48.7073	91.9409	3.9866	18.4740	47.4173	90.6039
	C_B	0.9138	0.9871	0.9954	0.9976	0.9433	0.9868	0.9948	0.9973	0.9212	0.9834	0.9937	0.9967
	C_F	0.0862	0.0129	0.0046	0.0024	0.0567	0.0132	0.0052	0.0027	0.0788	0.0166	0.0063	0.0033
	NF_2	3.6810	22.1734	61.8144	120.9939	4.7559	19.6231	48.5461	91.6190	3.9769	18.4150	47.2536	90.2784
2	NF_1	4.1386	22.6100	62.2482	121.4421	5.1564	20.0734	49.0906	92.3244	4.4368	18.9366	47.8716	91.0626
	C_B	0.7279	0.9503	0.9820	0.9904	0.8078	0.9491	0.9796	0.9891	0.7474	0.9366	0.9752	0.9868
	C_F	0.2721	0.0497	0.0180	0.0096	0.1922	0.0509	0.0204	0.0109	0.2526	0.0634	0.0248	0.0132
	NF_2	4.1315	22.5995	62.2395	121.4339	5.1457	20.0100	48.9236	91.9971	4.4235	18.8697	47.7008	90.7307
3	NF_1	4.7985	23.3152	62.9598	122.1807	5.7458	20.7121	49.7226	92.9597	5.0927	19.6839	48.6190	91.8216
	C_B	0.5472	0.8948	0.9604	0.9787	0.6554	0.8923	0.9553	0.9759	0.5737	0.8679	0.946	0.9709
	C_F	0.4528	0.1052	0.0396	0.0213	0.3446	0.1077	0.0447	0.0241	0.4263	0.1321	0.054	0.0291
	NF_2	4.7850	23.2922	62.9408	122.1633	5.7318	20.6389	49.5461	92.6236	5.0748	19.6044	48.4365	91.4790
4	NF_1	5.5861	24.2682	63.9414	123.2063	6.4726	21.5749	50.5939	93.8415	5.8788	20.6852	49.6456	92.8730
	C_B	0.4110	0.8272	0.9318	0.9629	0.5236	0.8234	0.9232	0.9580	0.4395	0.7871	0.908	0.9494
	C_F	0.5890	0.1728	0.0682	0.0371	0.4764	0.1766	0.0768	0.0420	0.5605	0.2129	0.092	0.0506
	NF_2	5.5662	24.2287	63.9083	123.1761	6.4554	21.4888	50.4042	93.4933	5.8564	20.5892	49.4472	92.5158
5	NF_1	6.4506	25.4407	65.1794	124.5109	7.2901	22.6360	51.6918	94.9627	6.7434	21.9053	50.9338	94.2064
	C_B	0.3165	0.7541	0.8976	0.9433	0.4217	0.7492	0.8851	0.9359	0.3446	0.7033	0.8635	0.9233
	C_F	0.6835	0.2459	0.1024	0.0567	0.5783	0.2508	0.1149	0.0641	0.6554	0.2967	0.1365	0.0767
	NF_2	6.4246	25.3814	65.1286	124.4644	7.2700	22.5344	51.4856	94.5989	6.7170	21.7900	50.7153	93.8305
6	NF_1	7.3614	26.8035	66.6579	126.0844	8.1663	23.8684	53.0019	96.3142	7.6551	23.3093	52.4633	95.8090
	C_B	0.2518	0.6809	0.8592	0.9205	0.3462	0.6752	0.8427	0.9103	0.2787	0.6227	0.815	0.8933
	C_F	0.7482	0.3191	0.1408	0.0795	0.6538	0.3248	0.1573	0.0897	0.7213	0.3773	0.185	0.1067
	NF_2	7.3299	26.7218	66.5860	126.0184	8.1436	23.7495	52.7760	95.9318	7.6252	23.1722	52.2210	95.4108
7	NF_1	8.3006	28.3282	68.3595	127.9156	9.0804	25.2461	54.5081	97.8861	8.5956	24.8647	54.2124	97.6666
	C_B	0.2068	0.6113	0.8183	0.8950	0.2907	0.6051	0.7977	0.8819	0.2323	0.549	0.7644	0.8604
	C_F	0.7932	0.3887	0.1817	0.1050	0.7093	0.3949	0.2023	0.1181	0.7677	0.451	0.2356	0.1396
	NF_2	8.2640	28.2222	68.2636	127.8269	9.0557	25.1085	54.2598	97.4819	8.5625	24.7045	53.9430	97.2424
8	NF_1	9.2578	29.9892	70.2661	129.9919	10.0193	26.7454	56.1941	99.6672	9.5540	26.5437	56.1595	99.7637
	C_B	0.1747	0.5473	0.7759	0.8675	0.2493	0.5410	0.7516	0.8513	0.1987	0.4838	0.7137	0.8254
	C_F	0.8253	0.4527	0.2241	0.1325	0.7507	0.4590	0.2484	0.1487	0.8013	0.5162	0.2863	0.1746
	NF_2	9.2165	29.8574	70.1434	129.8776	9.9930	26.5882	55.9206	99.2384	9.5181	26.3592	55.8598	99.3101
9	NF_1	10.2266	31.7641	72.3593	132.2998	10.9747	28.3459	58.0433	101.6458	10.5239	28.3227	58.2833	102.084
	C_B	0.1511	0.4898	0.7333	0.8385	0.2178	0.4837	0.7057	0.8193	0.1736	0.4272	0.6642	0.7893
	C_F	0.8489	0.5102	0.2667	0.1615	0.7822	0.5163	0.2943	0.1807	0.8264	0.5728	0.3358	0.2107
	NF_2	10.1810	31.6052	72.2073	132.1573	10.9472	28.1684	57.7423	101.1895	10.4856	28.1132	57.9505	101.5980
10	NF_1	11.2032	33.6336	74.6214	134.8255	11.9415	30.0299	60.0399	103.8098	11.5015	30.1827	60.5639	104.612
	C_B	0.1332	0.4389	0.6914	0.8084	0.1934	0.4333	0.6608	0.7863	0.1543	0.3787	0.6167	0.7528
	C_F	0.8668	0.5611	0.3086	0.1916	0.8066	0.5667	0.3392	0.2137	0.8457	0.6213	0.3833	0.2472
	NF_2	11.1535	33.4468	74.4377	134.6522	11.9129	29.8319	59.7091	103.3234	11.4609	29.9478	60.1954	104.0900

Table 4. Variation in strain and kinetic energies at fundamental frequencies of rotating double-tapered beam with clamped-free end condition: $c = 0.5$, $\bar{r}_H = 0$.

$\bar{\Omega}$	Total strain and kinetic energy							
	$\bar{\omega}_l$ (TMM)	U	T	$\bar{\omega}_l (\sqrt{U/T})$	U_B	U_F	C_B	C_F
0	4.62515	17.9617004	0.8422753	4.61792	17.96170	0.00000	1.0000	0.0000
1	4.76405	16.8709947	0.7459035	4.75586	15.91511	0.95589	0.9433	0.0567
2	5.15641	14.2614472	0.5386075	5.14571	11.52083	2.74062	0.8078	0.1922
3	5.74578	11.3203096	0.3445644	5.73184	7.41938	3.90092	0.6554	0.3446
4	6.47262	8.7652905	0.2103395	6.45539	4.58936	4.17593	0.5236	0.4764
5	7.29014	6.7788408	0.1282595	7.26997	2.85883	3.92001	0.4217	0.5783
6	8.16629	5.2981759	0.0798893	8.14365	1.83447	3.46371	0.3462	0.6538
7	9.08035	4.2046062	0.0512721	9.05570	1.22208	2.98252	0.2907	0.7093
8	10.01925	3.3918940	0.0339665	9.99299	0.84543	2.54646	0.2493	0.7507
9	10.97472	2.7800189	0.0231976	10.94717	0.60555	2.17447	0.2178	0.7822
10	11.94149	2.3121635	0.0162923	11.91291	0.44727	1.86490	0.1934	0.8066

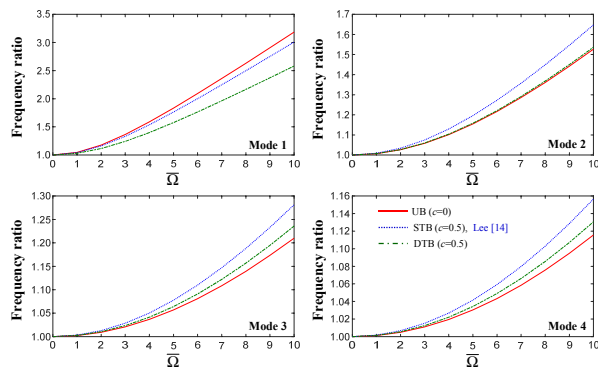


Fig. 4. Comparisons of frequency ratios at nondimensional natural frequencies of the three beam types owing to centrifugal stiffening.

trifugal force on the frequency ratio is limited. Other physical phenomena cannot be identified without considering the variation in the strain energy.

To identify various physical phenomena, Table 4 lists, as an example, the total strain and kinetic energies for the fundamental frequency of a rotating double-tapered beam with increasing rotational speed.

The total strain and kinetic energies presented in Table 4 can be computed using Eqs. (1) and (2). The strain and kinetic energy ratios are presented in Fig. 5(a). The total, bending, and additional strain energies generated by the centrifugal force are illustrated in Fig. 5(b). The total strain and kinetic energies owing to centrifugal stiffening decrease. However, the fundamental frequencies caused by these effects increase because the reduction in the total strain energies is smaller than that in the total kinetic energies. The bending strain energies caused by centrifugal stiffening are reduced substantially. Meanwhile, the additional strain energy generated by centrifugal stiffening, which is affected by the decrease in the total strain energies, increase and then decrease. Various physical phenomena that are yet to be identified can be detected based on the variations

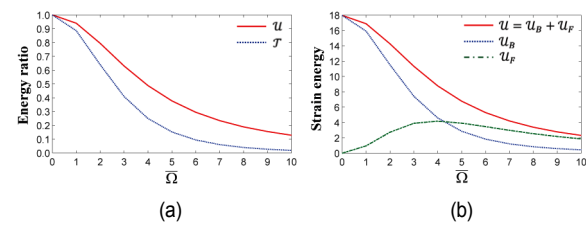


Fig. 5. Variations in strain and kinetic energies at fundamental frequencies of rotating double-tapered beam as function of rotational speed: (a) Total strain and kinetic energy ratio; (b) bending strain energy and additional strain energy owing to centrifugal stiffening.

in the strain and kinetic energies, using this method.

3.2 Effects of taper ratio and hub radius

The effects of the tapered ratio and hub radius on the non-dimensional natural frequencies of a rotating double-tapered beam with a cantilever end condition are analyzed in this subsection. The contribution rates of the strain energies with increasing hub radius are listed in Table 5. Fig. 6 illustrates the variations in the frequency ratio at the first four nondimensional natural frequencies of the rotating double-tapered beam as a function of the rotational speed.

Fig. 7 presents the variations in the contribution ratio of the strain energies for the first four nondimensional natural frequencies of the rotating double-tapered beam as a function of the rotational speed. Moreover, nondimensional hub radii of 0.5 and 1 are selected to analyze the effects on the eigenfrequencies. The contribution rates of the additional strain energy generated by centrifugal stiffening are increased substantially owing to the increase in the hub radii, whereas the contribution rates of the bending strain energies are decreased substantially.

To analyze the effect of the hub radius based on the variation in the total strain and kinetic energies, Tables 6 and 7

Table 5. Contribution rates of the strain energy on the nondimensional natural frequency of a rotating double-tapered beam varying by the increase in the hub radius.

$\bar{\Omega}$	Non-dimensional natural frequency and contribution rate							
	$c = 0.5, \bar{r}_H = 0.5$				$c = 0.5, \bar{r}_H = 1$			
	$\bar{\omega}_1$	$\bar{\omega}_2$	$\bar{\omega}_3$	$\bar{\omega}_4$	$\bar{\omega}_1$	$\bar{\omega}_2$	$\bar{\omega}_3$	$\bar{\omega}_4$
0	NF_1	4.6252	19.5476	48.5789	91.8128	4.6252	19.5476	48.5789
	C_B	1.0000	1.0000	1.0000	1.0000	1.0000	1.0000	1.0000
	C_F	0.0000	0.0000	0.0000	0.0000	0.0000	0.0000	0.0000
	NF_2	4.6179	19.4924	48.4196	91.4926	4.6179	19.4924	48.4196
1	NF_1	4.8555	19.7687	48.7962	92.0318	4.9451	19.8567	48.8850
	C_B	0.9087	0.9781	0.9913	0.9953	0.8765	0.9696	0.9877
	C_F	0.0913	0.0219	0.0087	0.0047	0.1235	0.0304	0.0123
	NF_2	4.8464	19.7100	48.6336	91.7086	4.9353	19.7966	48.7210
2	NF_1	5.4855	20.4177	49.4423	92.6856	5.7953	20.7562	49.7914
	C_B	0.7156	0.9178	0.9660	0.9816	0.6427	0.8886	0.9527
	C_F	0.2844	0.0822	0.0340	0.0184	0.3573	0.1114	0.0473
	NF_2	5.4720	20.3488	49.2699	92.3532	5.7793	20.6820	49.6136
3	NF_1	6.3909	21.4560	50.5000	93.7644	6.9748	22.1743	51.2646
	C_B	0.5333	0.8324	0.9266	0.9595	0.4508	0.7802	0.8997
	C_F	0.4667	0.1676	0.0734	0.0405	0.5492	0.2198	0.1003
	NF_2	6.3720	21.3712	50.3116	93.4170	6.9517	22.0784	51.0646
4	NF_1	7.4642	22.8301	51.9430	95.2529	8.3351	24.0177	53.2552
	C_B	0.3990	0.7368	0.8768	0.9303	0.3243	0.6671	0.8350
	C_F	0.6010	0.2632	0.1232	0.0697	0.6757	0.3329	0.1650
	NF_2	7.4400	22.7248	51.7328	94.8848	8.3054	23.8947	53.0251
5	NF_1	8.6364	24.4825	53.7388	97.1309	9.7940	26.1946	55.7044
	C_B	0.3071	0.6424	0.8203	0.8954	0.2440	0.5631	0.7649
	C_F	0.6929	0.3576	0.1797	0.1046	0.7560	0.4369	0.2351
	NF_2	8.6075	24.3534	53.5015	96.7366	9.7582	26.0406	55.4374
6	NF_1	9.8676	26.3593	55.8515	99.3748	11.3087	28.6259	58.5510
	C_B	0.2445	0.5562	0.7608	0.8563	0.1918	0.4741	0.6942
	C_F	0.7555	0.4438	0.2392	0.1437	0.8082	0.5259	0.3058
	NF_2	9.8344	26.2041	55.5825	98.9491	11.2673	28.4384	58.2410
7	NF_1	11.1349	28.4140	58.2447	101.9583	12.8567	31.2492	61.7361
	C_B	0.2009	0.4810	0.7012	0.8145	0.1564	0.4008	0.6267
	C_F	0.7991	0.5190	0.2988	0.1855	0.8436	0.5992	0.3733
	NF_2	11.0978	28.2312	57.9397	101.4966	12.8100	31.0266	61.3779
8	NF_1	12.4253	30.6088	60.8832	104.8544	14.4255	34.0173	65.2064
	C_B	0.1696	0.4170	0.6435	0.7713	0.1314	0.3413	0.5642
	C_F	0.8304	0.5830	0.3565	0.2287	0.8686	0.6587	0.4358
	NF_2	12.3848	30.3973	60.5384	104.3521	14.3739	33.7584	64.7953
9	NF_1	13.7311	32.9138	63.7344	108.0357	16.0081	36.8953	68.9153
	C_B	0.1464	0.3633	0.5891	0.7279	0.1131	0.2934	0.5078
	C_F	0.8536	0.6367	0.4109	0.2721	0.8869	0.7066	0.4922
	NF_2	13.6872	32.6728	63.3464	107.4886	15.9516	36.5992	68.4471
10	NF_1	15.0474	35.3057	66.7689	111.4754	17.6001	39.8574	72.8229
	C_B	0.1286	0.3186	0.5389	0.6852	0.0992	0.2546	0.4576
	C_F	0.8714	0.6814	0.4611	0.3148	0.9008	0.7454	0.5424
	NF_2	15.0004	35.0347	66.3349	110.8795	17.5390	39.5236	72.2940

Table 6. Variation in strain and kinetic energies at fundamental frequencies of rotating double-tapered beam with clamped-free end condition: $c = 0.5$, $\bar{r}_H = 0.5$.

$\bar{\Omega}$	Total strain and kinetic energy							
	$\bar{\omega}_l$ (TMM)	U	T	$\bar{\omega}_l (= \sqrt{U/T})$	U_B	U_F	C_B	C_F
0	4.62515	17.9617004	0.8422753	4.61792	17.96170	0.00000	1.0000	0.0000
1	4.85546	16.2201853	0.6905779	4.84643	14.73861	1.48158	0.9087	0.0913
2	5.48547	12.5452335	0.4189778	5.47197	8.97734	3.56789	0.7156	0.2844
3	6.39085	9.0769002	0.2235583	6.37196	4.84042	4.23648	0.5333	0.4667
4	7.46418	6.5192458	0.1177739	7.44002	2.60085	3.91839	0.3990	0.6010
5	8.63641	4.7691271	0.0643706	8.60748	1.46452	3.30461	0.3071	0.6929
6	9.86755	3.5811406	0.0370280	9.83435	0.87566	2.70548	0.2445	0.7555
7	11.13489	2.7610671	0.0224181	11.09785	0.55480	2.20627	0.2009	0.7991
8	12.42534	2.1807990	0.0142181	12.38475	0.36989	1.81091	0.1696	0.8304
9	13.73110	1.7594339	0.0093917	13.68721	0.25752	1.50191	0.1464	0.8536
10	15.04742	1.4458555	0.0064257	15.00037	0.18594	1.25991	0.1286	0.8714

Table 7. Variation in strain and kinetic energies at fundamental frequencies of rotating double-tapered beam with clamped-free end condition: $c = 0.5$, $\bar{r}_H = 1$.

$\bar{\Omega}$	Total strain and kinetic energy							
	$\bar{\omega}_l$ (TMM)	U	T	$\bar{\omega}_l (= \sqrt{U/T})$	U_B	U_F	C_B	C_F
0	4.62515	17.9617004	0.8422753	4.61792	17.96170	0.00000	1.0000	0.0000
1	4.94514	15.6170012	0.6411690	4.93529	13.68806	1.92894	0.8765	0.1235
2	5.79534	11.1930594	0.3351131	5.77935	7.19433	3.99873	0.6427	0.3573
3	6.97475	7.5674530	0.1565898	6.95173	3.41137	4.15609	0.4508	0.5492
4	8.33512	5.1809310	0.0751080	8.30540	1.68023	3.50070	0.3243	0.6757
5	9.79404	3.6714974	0.0385568	9.75823	0.89590	2.77559	0.2440	0.7560
6	11.30874	2.6994867	0.0212637	11.26733	0.51779	2.18170	0.1918	0.8082
7	12.85667	2.0519357	0.0125044	12.81004	0.32101	1.73092	0.1564	0.8436
8	14.42549	1.6048176	0.0077674	14.37387	0.21095	1.39387	0.1314	0.8686
9	16.00806	1.2856947	0.0050527	15.95164	0.14540	1.14030	0.1131	0.8869
10	17.60010	1.0511477	0.0034171	17.53899	0.10423	0.94692	0.0992	0.9008

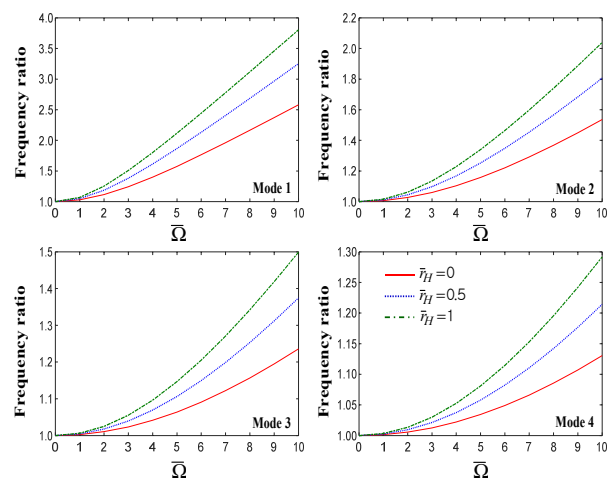


Fig. 6. Variations in frequency ratio at first four nondimensional natural frequencies of rotating double-tapered beam expressed as a function of rotational speed.

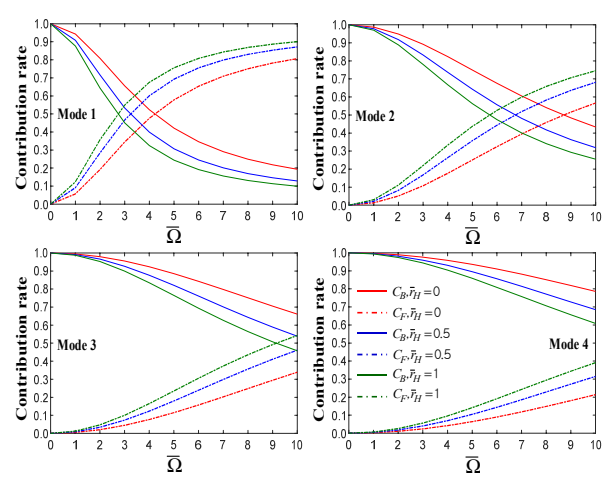


Fig. 7. Variations in contribution rate of strain energies at first four nondimensional natural frequencies of rotating double-tapered beam expressed as a function of rotational speed.

Table 8. Contribution rates of the strain energy on the first four nondimensional natural frequency of a rotating double-tapered beam varying by the increase of taper ratio.

<i>c</i>	Non-dimensional natural frequency and contribution rate								
	$\bar{\Omega} = 5, \bar{r}_H = 0$				$\bar{\Omega} = 10, \bar{r}_H = 0$				
	$\bar{\omega}_1$	$\bar{\omega}_2$	$\bar{\omega}_3$	$\bar{\omega}_4$	$\bar{\omega}_1$	$\bar{\omega}_2$	$\bar{\omega}_3$	$\bar{\omega}_4$	
0.0	NF_1	6.4506	25.4407	65.1794	124.5109	11.2032	33.6336	74.6214	134.8255
	C_B	0.3165	0.7541	0.8976	0.9433	0.1332	0.4389	0.6914	0.8084
	C_F	0.6835	0.2459	0.1024	0.0567	0.8668	0.5611	0.3086	0.1916
	NF_2	6.4246	25.3814	65.1286	124.4644	11.1535	33.4468	74.4377	134.6522
0.1	NF_1	6.5633	24.9029	62.6152	118.9542	11.3017	32.9554	71.8405	128.9685
	C_B	0.3325	0.7529	0.8958	0.9423	0.1417	0.4370	0.6867	0.8055
	C_F	0.6675	0.2471	0.1042	0.0577	0.8583	0.5630	0.3133	0.1945
	NF_2	6.5377	24.8349	62.5343	118.8462	11.2544	32.7651	71.6295	128.7374
0.2	NF_1	6.6969	24.3478	59.9763	113.2131	11.4188	32.2499	68.9817	122.9266
	C_B	0.3506	0.7518	0.8937	0.9412	0.1516	0.4354	0.6814	0.8019
	C_F	0.6494	0.2482	0.1063	0.0588	0.8484	0.5646	0.3186	0.1981
	NF_2	6.6719	24.2710	59.8647	113.0427	11.3746	32.0563	68.7422	122.6356
0.3	NF_1	6.8563	23.7819	57.2815	107.3213	11.5589	31.5244	66.0667	116.7385
	C_B	0.3711	0.7508	0.8913	0.9398	0.1631	0.4342	0.6754	0.7977
	C_F	0.6289	0.2492	0.1087	0.0602	0.8369	0.5658	0.3246	0.2023
	NF_2	6.8322	23.6966	57.1389	107.0879	11.5187	31.3282	65.7979	116.3854
0.4	NF_1	7.0498	23.2088	54.5230	101.2505	11.7295	30.7818	63.0886	110.3778
	C_B	0.3946	0.7499	0.8885	0.9381	0.1768	0.4334	0.6686	0.7927
	C_F	0.6054	0.2501	0.1115	0.0619	0.8232	0.5666	0.3314	0.2073
	NF_2	7.0272	23.1152	54.3489	100.9529	11.6942	30.5840	62.7894	109.9600
0.5	NF_1	7.2901	22.6360	51.6918	94.9627	11.9415	30.0299	60.0399	103.8098
	C_B	0.4217	0.7492	0.8851	0.9359	0.1934	0.4333	0.6608	0.7863
	C_F	0.5783	0.2508	0.1149	0.0641	0.8066	0.5667	0.3392	0.2137
	NF_2	7.2700	22.5344	51.4856	94.5989	11.9129	29.8319	59.7091	103.3234
0.6	NF_1	7.5972	22.0803	48.7797	88.4052	12.2119	29.2867	56.9143	96.9873
	C_B	0.4537	0.7489	0.8811	0.9331	0.2140	0.4341	0.6517	0.7783
	C_F	0.5463	0.2511	0.1189	0.0669	0.7860	0.5659	0.3483	0.2217
	NF_2	7.5810	21.9720	48.5408	87.9722	12.1924	29.0915	56.5513	96.4269
0.7	NF_1	8.0043	21.5823	45.7865	81.5048	12.5679	28.5962	53.7154	89.8452
	C_B	0.4924	0.7493	0.8760	0.9292	0.2402	0.4365	0.6409	0.7676
	C_F	0.5076	0.2507	0.1240	0.0708	0.7598	0.5635	0.3591	0.2324
	NF_2	7.9946	21.4705	45.5149	80.9979	12.5613	28.4104	53.3212	89.2037
0.8	NF_1	8.5700	21.2521	42.7558	74.1671	13.0550	28.0752	50.4956	82.3057
	C_B	0.5405	0.7517	0.8697	0.9238	0.2751	0.4420	0.6281	0.7530
	C_F	0.4595	0.2483	0.1303	0.0762	0.7249	0.5580	0.3719	0.2470
	NF_2	8.5721	21.1468	42.4561	73.5804	13.0675	27.9163	50.0797	81.5756
0.9	NF_1	9.4021	21.4619	40.0148	66.4099	13.7492	28.0899	47.6073	74.4290
	C_B	0.6029	0.7610	0.8624	0.9155	0.3238	0.4577	0.6146	0.7319
	C_F	0.3971	0.2390	0.1376	0.0845	0.6762	0.5423	0.3854	0.2681
	NF_2	9.4256	21.4038	39.7293	65.7615	13.7896	28.0149	47.2360	73.6389

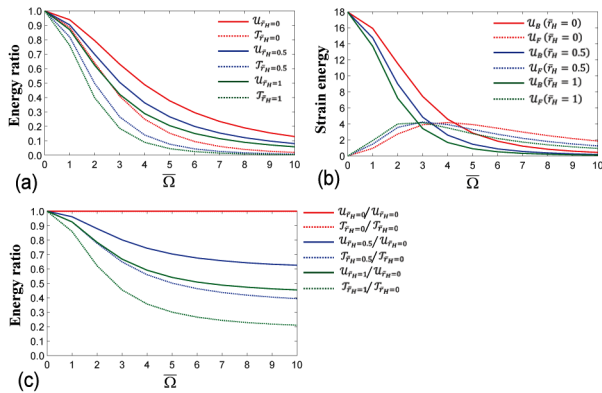


Fig. 8. Variations in strain and kinetic energies at fundamental frequency of rotating double-tapered beam owing to effect of hub radii: (a) Total strain and kinetic energy ratio; (b) bending and additional strain energies owing to centrifugal stiffening; (c) total strain and kinetic energy ratio for $\bar{r}_H = 0.5$ and 1 divided by $\bar{r}_H = 0$ at each rotational speed.

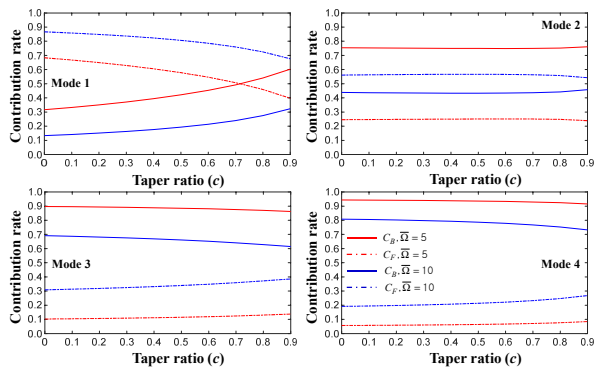


Fig. 9. Variations in contribution rate of strain energies at first four nondimensional natural frequencies of rotating double-tapered beam expressed as a function of taper ratio.

present, as an example, the total strain and kinetic energies for the fundamental frequency of a rotating double-tapered beam as a function of the rotational speed. The selected hub radii are $\bar{r}_H = 0, 0.5$, and 1.

Fig. 8 presents the variations in the strain and kinetic energies at the fundamental frequency of a rotating double-tapered beam with respect to the hub radius, based on Tables 4, 6, and 7.

In Fig. 8(a), the total energies decrease substantially as the hub radius increases. Furthermore, in Fig. 8(b), the bending strain energies caused by centrifugal stiffening decrease substantially as the hub radius increases. The additional strain energy generated by centrifugal stiffening increases and then decreases. Fig. 8(c) presents the variations in the total strain and kinetic energy ratio for each rotational speed. The larger the hub radius, the larger is the negative slope of the total energy ratio. Table 8 lists the contribution rates of the strain energy as the taper ratio increases, for the first four nondimensional natural frequencies of a rotating double-tapered beam at constant rotational speed. The rotational speeds $\bar{\Omega} = 5$ and 10 are selected. Moreover, Fig. 9 presents the variations in the contribution ratio of the strain energies at the first four nondimensional

natural frequencies of a rotating double-tapered beam with respect to the taper ratio. When the taper ratio increases, the contribution rates of the additional strain energies generated by centrifugal stiffening at the first and second nondimensional natural frequencies decrease, whereas the contribution rates at the third and four eigenfrequencies increase. In particular, the variations in the contribution rates caused by the centrifugal forces at the fundamental frequency are larger at a rotation speed of 5 than at 10.

As illustrated by the results, the investigation of energy variations is effective for identifying various physical phenomena caused by the dynamic behaviors of rotating double-tapered beams.

4. Conclusions

A transfer matrix expression was developed to investigate the effect of centrifugal forces on the natural frequencies of a rotating double-tapered beam. The effect of centrifugal stiffening was analyzed in terms of the contribution rates by employing the developed TMM. The stronger the effect of the centrifugal force, the lower are the total strain and kinetic energies. However, the natural frequencies caused by the increasing centrifugal force increased substantially. The present method is limited in practical engineering applications because it does not consider both rotary inertia and shear deformation. Nevertheless, the results are likely to be effective. Furthermore, the analytical method may aid in identifying other physical phenomena with regard to the dynamic behavior of rotating double-tapered beams.

Acknowledgments

The authors gratefully acknowledge the financial support for this research from the National Research Foundation of Korea (Grant number NRF-2018R1D1A1B07047019).

Nomenclature

$w(x, t)$: Bending displacement
$\zeta (= cx / L)$: Nondimensional variable
U	: Strain energy
T	: Kinetic energy
$EI(x)$: Bending stiffness varying by tapering
$EI(x)$: Bending stiffness of a uniform beam
$EI(x)$: Mass per unit length varying by tapering
m_0	: Mass per unit length when $c = 0$
ω	: Angular frequency
c	: Taper ratio
a_{i+1}	: Coefficients of the Frobenius series
$F(x)$: Centrifugal force
A	: Matrix for arbitrary constants
C	: Matrix for the state quantity at the start point
Q	: Matrix for the state quantity at the end point
T	: Transfer matrix

Z_0, Z_1	: Matrix for the state vectors
$f(\zeta, k)$: Function of the Frobenius series
r_H	: Hub radius
Φ	: Slope of the deformation curve
$M(x, t)$: Bending moment
$V(x, t)$: Shear force
S_B	: Bending strain energy
S_F	: Additional strain energy by the centrifugal force
C_B	: Contribution rate of the bending strain energy
C_F	: Contribution rate of the additional strain energy by the centrifugal force
U_{\max}	: Maximum strain energy
Ω	: Rotational angular speed
$\bar{\Omega}$: Nondimensional rotation speed
$\bar{\omega}$: Nondimensional natural frequency
T_{\max}	: Maximum kinetic energy

References

- [1] S. Wan, J. Hong, F. Du, B. Fang and X. Li, Modelling and characteristic investigation of spindle-holder assembly under clamping and centrifugal forces, *Journal of Mechanical Science and Technology*, 33 (5) (2019) 2397-2405.
- [2] P. A. Roy and S. A. Meguid, Analytical modeling of the coupled free vibration response of a rotating blade in a gas turbine engine, *Acta Mechanica*, 229 (8) (2018) 3355-3373.
- [3] X. Rui, L. K. Abbas, F. Yang, G. Wang, H. Yu and Y. Wang, Flapwise vibration computations of coupled helicopter rotor/fuselage: Application of multibody system dynamics, *AIAA Journal*, 56 (2) (2018) 818-835.
- [4] Z. Wang and R. Li, Transverse vibration of rotating tapered cantilever beam with hollow circular cross-section, *Shock and Vibration*, 2018 (2018).
- [5] D. I. Shin, S. M. Choi, G. W. Jang and Y. Y. Kim, Finite element beam analysis of tapered thin-walled box beams, *Thin-Walled Structures*, 102 (2016) 205-214.
- [6] H. Liu, Z. Wei, G. Tan, Y. Han and Z. Liu, Vibratory characteristics cracked non-uniform beams with different boundary conditions, *Journal of Mechanical Science and Technology*, 33 (1) (2019) 377-392.
- [7] R. D. Firouz-Abadi, M. Rahmanian and M. Amabili, Exact solutions for free vibrations and buckling of double tapered columns with elastic foundation and tip mass, *Journal of Vibration and Acoustics*, 135 (5) (2013) 051017.
- [8] A. Nikolic and S. Salinic, Buckling analysis of non-prismatic columns: A rigid multibody approach, *Engineering Structures*, 143 (2017) 511-521.
- [9] J. Tian, J. Su, K. Zhou and H. Hua, A modified variational method for nonlinear vibration analysis of rotating beams including Coriolis effects, *Journal of Sound and Vibration*, 426 (2018) 258-277.
- [10] G. Zhao and Z. Wu, Coupling vibration analysis of rotating three-dimensional cantilever beam, *Computers and Structures*, 179 (2017) 64-74.
- [11] Y. Zhou, Y. Zhang and G. Yao, Stochastic forced vibration analysis of a tapered beam with performance deterioration, *Acta Mechanica*, 228 (4) (2017) 1393-1406.
- [12] H. H. Yoo and S. H. Shin, Vibration analysis of rotating cantilever beams, *Journal of Sound and Vibration*, 212 (5) (1998) 807-828.
- [13] J. Chung and H. H. Yoo, Dynamic analysis of a rotating tapered beam by using the finite element method, *Journal of Sound and Vibration*, 249 (1) (2002) 147-164.
- [14] H. P. Lee, Effect of gravity on the stability of a rotating cantilever beam in a vertical plane, *Computers and Structures*, 53 (2) (1994) 351-355.
- [15] K. S. Bhat and R. Ganguli, Non-rotating beams isospectral to rotating Rayleigh beams, *International Journal of Mechanical Sciences*, 142-143 (2018) 440-455.
- [16] Y. A. Khulief and A. Bazoune, Frequencies of rotating tapered Timoshenko beams with different boundary conditions, *Computers and Structures*, 42 (5) (1992) 781-795.
- [17] A. Bazoune and Y. A. Khulief, A finite beam element for vibration analysis of rotating tapered Timoshenko beams, *Journal of Sound and Vibration*, 156 (1) (1992) 141-164.
- [18] T. Yokoyama, Free vibration characteristics of rotating Timoshenko beams, *International Journal of Mechanical Sciences*, 30 (10) (1988) 743-755.
- [19] B. G. Bazehhour, S. M. Mousavi and A. Farshidianfar, Free vibration of high-speed rotating Timoshenko shaft with various boundary conditions: Effect of centrifugally induced axial force, *Archive of Applied Mechanics*, 84 (12) (2014) 1691-1700.
- [20] A. Bazoune, Y. A. Kulief, N. G. Stephen and M. A. Mohiuddin, Dynamic response of spinning tapered Timoshenko beams using modal reduction, *Finite Elements in Analysis and Design*, 37 (3) (2001) 199-219.
- [21] Y. Chen, J. Zhang and H. Zhang, Free vibration analysis of rotating tapered Timoshenko beams via variational iteration method, *Journal of Vibration and Control*, 23 (2) (2017) 220-234.
- [22] Y. Huo and Z. Wang, Dynamic analysis of a rotating double-tapered cantilever Timoshenko beam, *Archive of Applied Mechanics*, 86 (6) (2016) 1147-1161.
- [23] O. Fakharian, H. Salmani and S. A. H. Kordkheili, A lumped parameter model for exponentially tapered piezoelectric beam in transverse vibration, *Journal of Mechanical Science and Technology*, 33 (5) (2019) 2043-2048.
- [24] K. Sarkar and R. Ganguli, Modal tailoring and closed-form solutions for rotating non-uniform Euler-Bernoulli beams, *International Journal of Mechanical Sciences*, 88 (2014) 208-220.
- [25] J. W. Lee and J. Y. Lee, A transfer matrix method for in-plane bending vibrations of tapered beams with axial force and multiple edge cracks, *Structural Engineering and Mechanics*, 66 (1) (2018) 125-138.
- [26] A. Keshmiri, N. Wu and Q. Wang, Vibration analysis of non-uniform tapered beams with nonlinear FGM properties, *Journal of Mechanical Science and Technology*, 32 (11) (2018) 5325-5337.
- [27] J. W. Lee and J. Y. Lee, In-plane bending vibration analysis of a rotating beam with multiple edge cracks by using the transfer

- matrix method, *Meccanica*, 52 (4-5) (2017) 1143-1157.
- [28] M. Bakhtiari, A. A. Lakis and Y. Kerboua, Nonlinear supersonic flutter of truncated conical shells, *Journal of Mechanical Science and Technology*, 34 (4) (2020) 1375-1388.
- [29] J. R. Banerjee and A. Ananthapuvirajah, Free flexural vibration of tapered beams, *Computers and Structures*, 224 (2019) 106106.
- [30] X. Yang, S. Wang and W. Zhang, Dynamic analysis of a rotating tapered cantilever Timoshenko beam based on the power series method, *Applied Mathematics and Mechanics-Engl. Ed.*, 38 (10) (2017) 1425-1438.
- [31] D. Adair and M. Jaeger, A power series solution for rotating nonuniform Euler-Bernoulli cantilever beams, *Journal of Vibration and Control*, 24 (17) (2018) 3855-3864.
- [32] J. R. Banerjee, Free vibration of centrifugally stiffened uniform and tapered beams using the dynamic stiffness method, *Journal of Sound and Vibration*, 233 (5) (2000) 857-875.
- [33] T. D. Chaudhari and S. K. Maiti, Modelling of transverse vibration of beam of linearly variable depth with edge crack, *Engineering Fracture Mechanics*, 63 (4) (1999) 425-445.
- [34] J. W. Lee and J. Y. Lee, Free vibration analysis using the transfer-matrix method on a tapered beam, *Computers and Structures*, 164 (2016) 75-82.
- [35] J. R. Banerjee, H. Su and D. R. Jackson, Free vibration of rotating tapered beams using the dynamic stiffness method, *Journal of Sound and Vibration*, 298 (4-5) (2006) 1034-1054.
- [36] S. Y. Lee, S. M. Lin and J. J. Hsu, In-plane vibration of a rotating curved beam with an elastically restrained root, *Journal of Sound and Vibration*, 315 (4-5) (2008) 1086-1102.
- [37] A. Y. Tang, X. F. Li, J. X. Wu and K. Y. Lee, Flapwise bending vibration of rotating tapered Rayleigh cantilever beams, *Journal of Constructional Steel Research*, 112 (2015) 1-9.
- [38] D. H. Hodges and M. J. Rutkowski, Free-vibration analysis of rotating beams by a variable-order finite element method, *AIAA Journal*, 19 (11) (1981) 1459-1466.
- [39] O. O. Ozgumus and M. O. Kaya, Flapwise bending vibration analysis of double tapered rotating Euler-Bernoulli beam by using the differential transform method, *Meccanica*, 41 (6) (2006) 661-670.
- [40] R. O. Stafford and V. Giurgiutiu, Semi-analytic methods for rotating Timoshenko beams, *International Journal of Mechanical Sciences*, 17 (11-12) (1975) 719-727.
- [41] J. W. Lee and J. Y. Lee, An exact transfer matrix expression for bending vibration analysis of a rotating tapered beam, *Applied Mathematical Modelling*, 53 (2018) 167-188.
- [42] J. W. Lee, J. H. Kwak and J. Y. Lee, Exact solution for bending vibration of rotating cantilever beam with tapered width using transfer matrix method, *The Korean Society for Noise and Vibration Engineering*, 26 (1) (2016) 75-81.



Jungwoo Lee received B.S., M.S., and Ph.D. degrees from Kyonggi University in 2002, 2004, and 2017, respectively. He is currently an Assistant Professor at the Department of Mechanical System Engineering of Kyonggi University. His research interests are in structural vibration, composite structures, continuum mechanics, and the transfer matrix method.



Jung Youn Lee is a Professor of Dept. of Mechanical System Engineering at Kyonggi University, where he has been since 1996. He received a B.S., an M.S. and his Ph.D. from Hanyang University in 1979, 1989 and 1992, respectively. His research interests are in system identification, structural modification, inverse problem, modal analysis and sensitivity analysis of vibration.